Phoenix: An Epidemic Approach to Time Reconstruction

Jayant Gupchup* Douglas Carlson* Răzvan Musăloiu-E.* Alex Szalay‡
Andreas Terzis*

Computer Science Department* Physics and Astronomy Department‡
Johns Hopkins University
{gupchup,carlsondc,razvanm,terzis}@jhu.edu* szalay@jhu.edu‡

Abstract. Harsh deployment environments and uncertain run-time conditions create numerous challenges for postmortem time reconstruction methods. For example, motes often reboot and thus lose their clock state, considering that the majority of mote platforms lack a real-time clock. While existing time reconstruction methods for long-term data gathering networks rely on a persistent basestation for assigning global timestamps to measurements, the basestation may be unavailable due to hardware and software faults. We present *Phoenix*, a novel offline algorithm for reconstructing global timestamps that is robust to frequent mote reboots and does not require a persistent global time source. This independence sets Phoenix apart from the majority of time reconstruction algorithms which assume that such a source is always available. Motes in Phoenix exchange their time-related state with their neighbors, establishing a chain of transitive temporal relationships to one or more motes with references to the global time. These relationships allow Phoenix to reconstruct the measurement timeline for each mote. Results from simulations and a deployment indicate that Phoenix can achieve timing accuracy up to 6 ppm for 99% of the collected measurements. Phoenix is able to maintain this performance for periods that last for months without a persistent global time source. To achieve this level of performance for the targeted environmental monitoring application, Phoenix requires an additional space overhead of 4% and an additional duty cycle of 0.2%.

1 Introduction

Wireless sensor networks have been used recently to understand spatiotemporal phenomena in environmental studies [12, 21]. The data these networks collect are scientifically useful only if the collected measurements have corresponding, accurate global timestamps. The desired level of accuracy in this context is in the order of milliseconds to seconds. In order to reduce complexity of the code running on the mote, it is more efficient to record sensor measurements using the mote's local time frame and perform a postmortem reconstruction to translate them to global time.

Each mote's clock (referred to as local clock henceforth) monotonically increases and resets to zero upon reboot. A naive postmortem time reconstruction

scheme collects $\langle local, global \rangle$ pairs during a mote's lifetime, using a global clock source (typically, an NTP-synchronized PC). These pairs (also referred to as "anchor points") are then used to translate the collected measurements to the global time frame by estimating the motes' clock skew and offset. We note that this methodology is unnecessary for architectures such as Fleck, which host a battery-backed on-board real-time clock (RTC) [4]. However, many commonly-used platforms such as Telos, Mica2, MicaZ, and IRIS (among others) lack an on-board RTC.

In the absence of reboots, naive time reconstruction strategies perform well. However, in practice, motes reboot due to low battery power, high moisture, and software defects. Even worse, when motes experience these problems, they may remain completely inactive for non-deterministic periods of time. Measurements collected during periods which lack $\langle local, global \rangle$ anchors (due to rapid reboots and/or basestation absence) are difficult or impossible to accurately reconstruct. Such situations are not uncommon based on our deployment experiences and those reported by others [22].

In this work, we devise a novel time reconstruction strategy, *Phoenix*, that is robust to random mote reboots and intermittent connection to the global clock source. Each mote periodically listens for its neighbors to broadcast their local clock values. These $\langle local, neighbor \rangle$ anchors are stored on the mote's flash. The system assumes that one or more motes can periodically obtain global time references, and they store these $\langle local, global \rangle$ anchors in their flash. When the basestation collects the data from these motes, an offline procedure converts the measurements timestamped using the motes' local clocks to the global time by using the transitive relationships between the local clocks and global time.

The offline nature of Phoenix has two advantages: **(a)** it reduces the complexity of the software running on the mote, and **(b)** it avoids the overhead associated with executing a continuous synchronization protocol. We demonstrate that Phoenix can reconstruct global timestamps accurately (within seconds) and achieve low ($< 1\%$) data losses in the presence of random mote reboots even when months pass without access to a global clock source.

2 Motivation

We claim that the problem of rebooting motes is a practical aspect of real deployments that has a high impact on environmental monitoring applications. We also quantify the frequency and impact of reboots in a long-term deployment. We begin by understanding why mote reboots complicate postmortem time reconstruction.

2.1 Postmortem Timestamp Reconstruction

The relationship between a mote's local clock, LTS, and the global clock, GTS, can be modeled with a simple linear relation: $GTS = \alpha \times LTS + \beta$, where α represents the mote's skew and β represents the intercept (global time when the

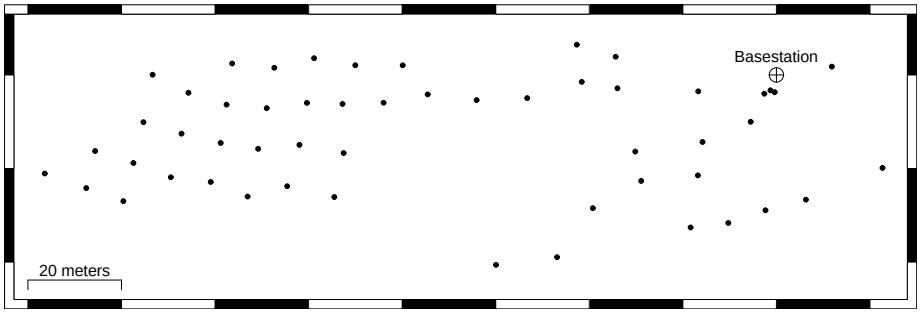

Fig. 1. The 53-mote "Cub Hill" topology, located in an urban forest northeast of Baltimore, Maryland.

mote reset its clock) [18]. This conversion from the local clock to global clock holds as long as the mote's local clock monotonically increases at a constant rate. We refer to this monotonically increasing period as a *segment*. When a mote reboots and starts a new segment, one needs to re-estimate the fit parameters. If a mote reboots multiple times while it is out of contact with the global clock source, estimating β for these segments is difficult. While data-driven treatments have proven useful for recovering temporal integrity, they cannot replace accurate timestamping solutions [9, 10]. Instead, time reconstruction techniques need to be robust to mote reboots and not require a persistent global time source.

2.2 Case Studies

We present two cases which illustrate the deployment problems that Phoenix intends to address. The first is an account of lessons learned from a year-long deployment of 53 motes. The second is a result of recent advances in solar-powered sensor networks.

Software Reboots. We present "Cub Hill", an urban forest deployment of 53 motes that has been active since July 2008 (Figure 1). Sensing motes collect measurements every 10 minutes to study the impact of land use on soil conditions. The basestation uses the Koala protocol to collect data from these motes every six hours [15]. We use TelosB motes driven by 19 Ah, 3.6 V batteries.

We noticed that motes with low battery levels and/or high internal moisture levels suffered from periodic reboots. As an example, Figure 2 shows the battery voltage of a mote that rebooted thrice in one month. Despite their instability, many of these motes were able to continue collecting measurements for extended periods of time.

Following a major network expansion, a software fault appeared which caused nodes to "freeze". Unable to reproduce this behavior in a controlled environment, we employed the MSP430's Watchdog Timer to reboot motes that enter this state [20]. While this prevented motes from completely failing, it also shortened

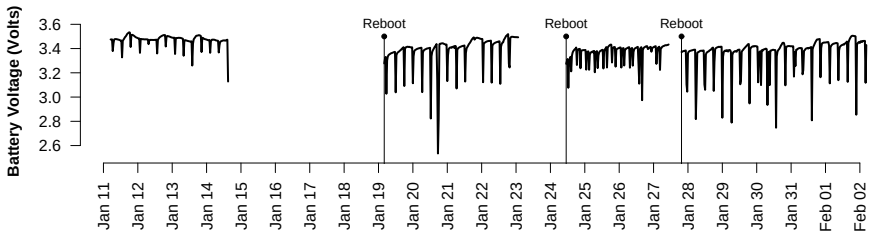

Fig. 2. An example of a mote rebooting due to low battery voltage (no watchdog timer in use). The sharp downward spikes correspond to gateway downloads (every six hours). Gaps in the series are periods where the mote was completely inoperative.

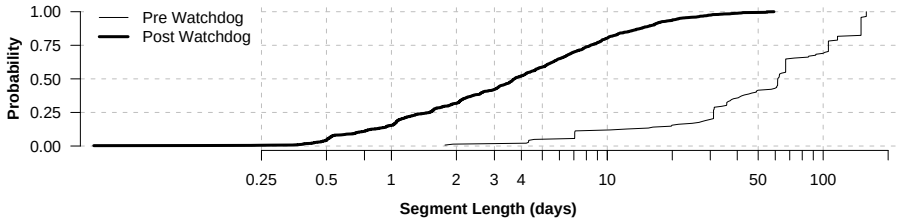

Fig. 3. The distribution of the segment lengths before and after adding the watchdog timer to the mote software.

the median length of the period between reboots from more than 50 days to only four days, as Figure 3 shows.

Solar Powered Sensor Networks. A number of research groups have demonstrated the use of solar energy as a means of powering environmental monitoring sensor networks [11, 19]. In such architectures, a mote can run out of power during cloudy days or at night. Motes naturally reboot in such architectures, and data losses are unavoidable due to the lack of energy. It is unclear how one can achieve temporal reliability without a persistent basestation or an on-board RTC. To the best of our knowledge, no one has addressed the issue of temporal integrity in solar-powered sensor networks. Yang et al. employ a model in which data collection happens without a persistent basestation [23]. The data upload takes place infrequently and opportunistically. Hard-to-predict reboot behavior is common to these systems. Furthermore, we note that even though there is very little information about the rate of reboots in such architectures, it is clear that such systems are susceptible to inaccurate timestamp assignments.

2.3 Impact

We evaluate the impact of mote reboots on the Cub Hill deployment using our existing time reconstruction methodology.

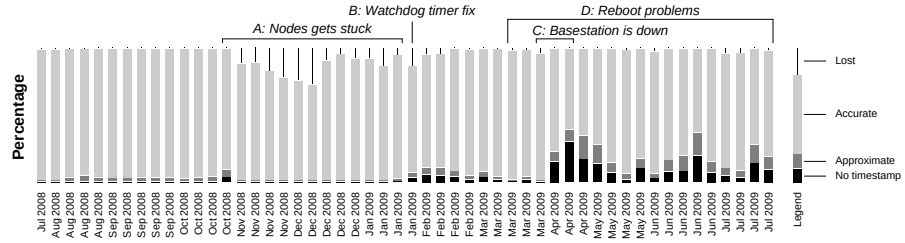

(a) The fraction of measurements that were assigned timestamps.

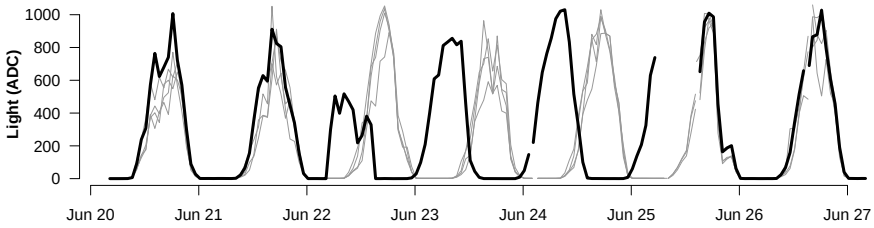

(b) An example of the impact of estimating β incorrectly when using approximate methods. Data from one of the motes (represented with the dark line) that rebooted multiple times between Jun. 22 and Jun. 25. During this period, the mote was out of sync with the rest (shown in gray) due to inaccurate β estimates

Fig. 4. Impact of time reconstruction methodology using the RGTR algorithm.

The basestation records an anchor point each time it downloads data from a mote. Motes that are poorly connected to the basestation may remain out of contact for several download rounds before connectivity improves and they can transfer their data. When motes reboot at a rate faster than the frequency with which the basestation contacts them, there exist periods which lack enough information to accurately reconstruct their measurement timestamps.

Upon acquiring the anchor points, the measurements are converted from their local clock to the global clock at the basestation. We employ our previously proposed algorithm, Robust Global Timestamp Reconstruction algorithm (referred to as RGTR), for this purpose [9]. We note that in order to estimate the fit parameters (α, β) for the segments, RGTR requires at least two anchor points. Depending on the accuracy requirements, one can assume that the skew (α) is stable per mote for small segments. Using this assumption, at least one anchor point is needed to estimate the β for any given segment, provided that α has been estimated accurately for the mote.

Figure 4(a) demonstrates the impact of mote reboots on time reconstruction for the Cub Hill deployment. During period A, motes were prone to freezing (and thus stopped sampling), leading to a decrease in the total data collected. At point B, the addition of the watchdog timer caused the total data collected to return to its previous level. However, due to the increased frequency of reboots, a larger portion of the samples could not be assigned a global timestamp (exacerbated by the absence of the base station during period C).

For segments where no anchor points were collected, we assumed that node reboots are instantaneous. However, this assumption does not always hold (see Figure 2) and leads to a small fraction of misaligned measurements. Figure 4(b) presents an example of this misalignment. One node (shown in bold) rebooted multiple times and could not reach the basestation during its active periods. The assumption of instantaneous reboots led to inaccurate β estimates.

3 Solution

Phoenix is a postmortem time reconstruction algorithm for motes operating without in-network time synchronization. It consists of two stages.

3.1 In-Network Anchor Collection

Each mote operates solely with respect to its own local clock. A new segment (uniquely identified by $\langle moteid, reboot\ count \rangle$) begins whenever a mote reboots: each segment starts at a different time and may run at a different rate. Our architecture assumes that there is at least one mote in the network that can periodically obtain references from an accurate global time source. This is done to establish the global reference points needed by Phoenix. This source may be absent for long periods of time (see Section 4). The global time source can be any reliable source (a mote equipped with a GPS receiver, NTP-synced basestation, etc). Without loss of generality, we assume that the network contains a mote connected to GPS device and a basestation that collects data infrequently[1].

All motes (including the GPS-connected mote) broadcast their local clock and reboot-count values every T_{beacon} seconds. Each receiving mote stores this information (along with its own local clock and reboot counter) in flash to form anchor records. The format of these records is $\langle moteid_r, rc_r, lc_r, moteid_s, rc_s, lc_s \rangle$; where rc, lc, r, and s refer to the reboot counter, local clock, receiver and sender respectively. Periodically, motes turn on their radios and listen for broadcasts in order to anchor their time frame to those of their neighbors. Each mote tries to collect this information from its neighbors after every reboot and after every T_{wakeup} seconds ($\gg T_{beacon}$). The intuition behind selecting this strategy is as follows. The reboot time determines the β parameter. The earliest opportunity to extract this information is immediately after a reboot. To get a good estimate of the skew, one would like to collect multiple anchors that are well distributed in time. Thus, T_{wakeup} is a parameter that governs how far to spread out anchor collections. In the case of a GPS mote, the $moteid_r, rc_r$ and $moteid_s, rc_s$ are identical, and lc_r, lc_s represent the local and global time respectively.

The basestation periodically downloads these anchors along with the measurements. This information is then used to assign global timestamps to the collected measurements using Algorithm 1. If the rate of reboots is known, the

[1] Note that the basestation collects data *only* and it does not provide a time source, unless specified otherwise.

Algorithm 1 Phoenix

Definitions:
a, b : alpha and beta for local-local fits;
P : parent segment; Π : Ancestor segments

procedure PHOENIX(AP)
  for each (i, j) in KEYS(AP) **do** ▷ All unique segment pairs in AP
    $LF_{a,b,\chi,df}(i, j) \leftarrow$ LLSE($AP(i, j)$) ▷ Compute the local-local fits
  for each $s \in S$ **do** ▷ Set of all unique segments
    $GF_{\alpha,\beta,P,\Pi,\chi,df}(s) \leftarrow (\emptyset, \emptyset, \emptyset, s, \chi_{MAX}, \emptyset)$ ▷ Initialize global fits
  for each $g \in G$ **do** ▷ All segments anchored to GTS
    INITGTSNODES(g, LF, GF)
    ENQUEUE(Q, g) ▷ Add all the GTS nodes to the queue
  while NOTEMPTY(Q) **do**
    $q \leftarrow$ DEQUEUE(Q)
    $C \leftarrow$ NEIGHBORANCHORS(q)
    for each $c \in C$ **do**
      $T_{\alpha,\beta,P,\Pi,\chi,df}(c) \leftarrow$GLOBALFIT($c, q, GF, LF$)
      if (UPDATEFIT(c, T, GF)) **then** ▷ Check for a better fit
        ENQUEUE(C)
  return GF

procedure INITGTSNODES(g, LF, GF)
  $GF(g) \leftarrow (LF_a(g, g'), LF_b(g, g'), \emptyset, g, LF_\chi(g, g'), LF_{df}(g, g'))$ ▷ g' is GTS, g is LTS

procedure GLOBALFIT(c, q, GF, LF)
  if $q > c$ **then** ▷ Smaller segment is the independent variable
    $\alpha_{new} \leftarrow GF_\alpha(q) * LF_a(q, c)$
    $\beta_{new} \leftarrow GF_\alpha(q) * LF_b(q, c) + GF_\beta(q)$
  else
    $\alpha_{new} \leftarrow GF_\alpha(q)/LF_a(q, c)$
    $\beta_{new} \leftarrow GF_\alpha(q) - \alpha_{new} * LF_b(q, c)$
  $\chi \leftarrow \frac{GF_{df}(q)*GF_\chi(q)+LF_{df}(q,c)*LF_\chi(q,c)}{GF_{df}(q)+LF_{df}(q,c)}$ ▷ Compute the weighted GOF metric.
  $df \leftarrow GF_{df}(q) + LF_{df}(q, c)$
  return $(\alpha_{new}, \beta_{new}, q, \{c \cup GF_\Pi(q)\}, \chi, df)$ ▷ Update parent/ancestors

procedure UPDATEFIT(c, T, GF)
  if $c \in T_\Pi(c)$ **then** ▷ Check for cycles
    return false
  if $T_\chi(c) < GF_\chi(c)$ **then**
    $GF_{\alpha,\beta,P,\Pi,\chi,df}(c) \leftarrow T_{\alpha,\beta,P,\Pi,\chi,df}(c)$
    return true
  else
    return false

anchor collection frequency can be fixed conservatively to collect enough anchors between reboots. One could also employ an adaptive strategy by collecting more anchors when the segment is small and reverting to a larger T_{wakeup} when an adequate number of anchors have been collected. It is advantageous for a mote to attempt to collect anchors from a small set of neighbors (to minimize storage), but this requires a mote to have some way of identifying the most useful segments for anchoring (see Section 4).

3.2 Offline Timestamp Reconstruction

The Phoenix algorithm is intuitively simple. We will outline it in text and draw attention to a few important details. For a more complete treatment, please refer to the pseudocode in Algorithm 1. Phoenix accepts as input the collection of all

anchor points AP (both $\langle local, neighbor \rangle$ and $\langle local, global \rangle$). It then employs a least-square linear regression to extract the relationships between the local clocks of the segments that have anchored to each other (LF, for Local Fit). In addition to $LF_a(i,j)$ (slope), $LF_b(i,j)$ (intercept), Phoenix also obtains a goodness-of-fit (GOF) metric, $LF_\chi(i,j)$ (unbiased estimate of the variance of the residuals) and LF_{df} (degrees of freedom). For segments which have global references, Phoenix stores this as GF (for Global Fit).

The algorithm then initializes a queue with all of the segments which have direct anchors to the global clock. It dequeues the first element q and examines each segment c that has anchored to it. Phoenix uses the transitive relationship between $GF(q)$ and $LF(q,c)$ to produce a global fit $T(c)$ which associates segment c to the global clock through segment q. If $T_\chi(c)$ is lower than the previous value for $GF_\chi(c)$ (and using q would not create a cycle in the path used to reach the global clock), the algorithm replaces $GF(c)$ with $T(c)$, and places c in the queue. When the queue is empty, no segments have "routes" to the global clock which have a better goodness-of-fit than the ones which have been previously established. At this point, the algorithm terminates.

The selection of paths from an arbitrary segment to a segment with global time references can be thought of as a shortest-path problem (each segment represents a vertex and the fit between the two segments is an edge). The GOF metric represents the edge weight. The running time complexity of the implementation of Phoenix was validated experimentally by varying the deployment lifetime (thereby varying number of segments). The runtime was found to increase slower than the square of the number of segments.

4 Evaluation

We evaluate the effect of varying several key parameters in Phoenix using both simulated and real datasets. We begin by describing our simulator.

4.1 Simulator

Our goal is to minimize the data loss in long-term deployments. Hence, we fix the simulation period to be one year. We also assume that the basestation is not persistently present and does not provide a time source to the network. The network contains one global clock source (a GPS mote) that is susceptible to failures. The main components of the simulator are described below. The default values for the simulator are based on empirical data obtained from the one year long Cub Hill deployment.

Clock Skew: The clock skew for each segment is drawn from a uniformly distributed random variable between 40 ppm and 70 ppm. Burri et al. report this value to be between 30 and 50 ppm at room temperature[2] [1].

[2] We ignore the well-studied temperature effects on the quartz crystal. For a more complete treatment on the temperature dependence, refer to [14, 16].

Segment Model: We use the non-parametric segment-length model based on the Cub Hill deployment after the watchdog timer fix (Figure 3). Additionally, after a reboot, we allowed the mote to stay inactive for a period that is randomly drawn between zero and four hours with a probability given by $p_{down} = 0.2$. The GPS mote's behavior follows the same model.
Communication Model: The total end-to-end communication delay for receiving anchor packets is drawn uniformly between 5 and 15 milliseconds. This time includes the interrupt handling, transmission, reception and propagation delays. To model the packet reception rate (PRR), we use the log-distance path loss model as described in [17, 24] with parameters: $(P_r(d_0), \eta, \sigma, d_0) = (-59.28, 2.04, 6.28, 2.0m)$.
Topology: The Cub Hill topology was used as the basis for all simulations.
Event Frequencies: Motes recorded a 26-byte sample every 10 minutes. They beacon their local clock values with an interval of T_{beacon}. They stay up after every reboot and periodically after an interval of T_{wakeup} to collect these broadcasts. While up, they keep their radios on for a maximum of T_{listen}. The GPS mote collects $\langle local, global \rangle$ anchors with a rate of T_{sync}. By default, T_{beacon}, T_{wakeup}, T_{listen} and T_{sync} were set to 30 s, 6 h, 30 s and 6 h respectively.
Maximum Anchorable Segments: To minimize the space overhead in storing anchors, we limit the number of segments that can be used for anchoring purposes. At any given time, a mote can only store anchors for up to $NUMSEG$ segments. The default $NUMSEG$ value is set to four. Motes stop listening early once they collect $NUMSEG$ anchors in a single interval.
Eviction Policy: Since segments end and links between motes change over time, obsolete or rarely-heard segments need to be evicted from the set of $NUMSEG$ segments for which a mote listens. The timeout for evicting stale entries is set to $3 \times T_{wakeup}$. We evaluated three different strategies for selecting replacements for evicted segments. First-come, first-served (FCFS) accepts the first segment that is heard when a vacancy exists. RAND keeps track of the previous segments that were heard and selects a new segment to anchor with at random. Longest local clock (LLC) keeps track of the local clock values of the segments that are heard and selects the segment that has the highest local clock. FCFS was chosen as the default.

4.2 Evaluation metrics

Data loss (DL): The fraction of data that cannot be assigned any timestamps, expressed as a percentage.
PPM Error: The average error (in parts per million) for the assigned timestamps. PPM error is $\frac{|t'-t|}{t_\delta} \times 10^6$, where t is the true timestamp of the measurement, t' is the assigned timestamp, and t_δ denotes the elapsed time since the start of the segment in terms of the real clock.
Space overhead: The fraction of space that is used for storing anchors relative to the total space used, expressed as a percentage.
Duty cycle: The fraction of time the radio was kept on for anchor collection and beaconing, expressed as a percentage.

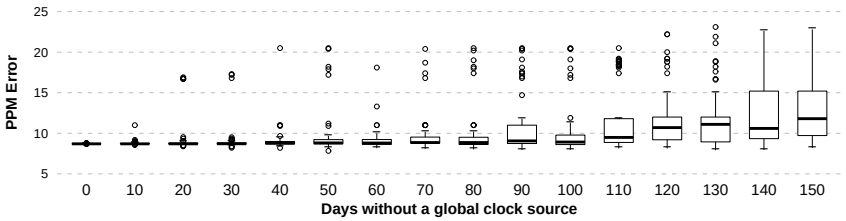

(a) The effect of a missing global clock source on accuracy.

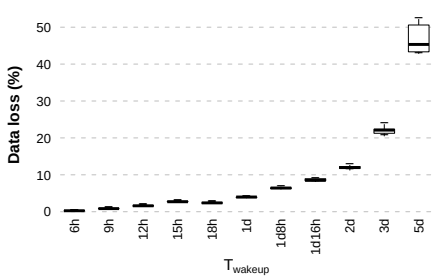

(b) The impact of T_{wakeup} on data loss.

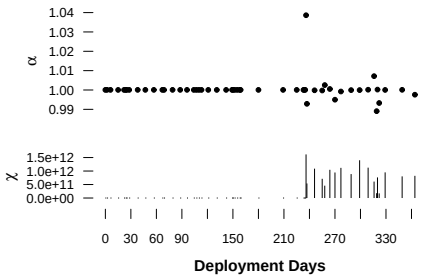

(c) Robustness to bad anchors.

Fig. 5. Evaluation of Phoenix in simulation. In (c), faults were injected to GPS anchors after day 237. Figure shows the α and χ values for the GPS mote for the entire period.

4.3 Simulation Experiments

Dependence on Global Clock Source: We studied the effect of the global clock's absence on data loss. We assume that the network contains one GPS mote that serves as the global clock source and it is inoperative for a specified amount of time. In order to avoid bias, we randomly selected the starting point of this period and varied the GPS down time from 0 to 150 days in steps of 10. Figure 5(a) shows the effect on the reconstruction using 60 independent runs. The accuracy decreases as the number of days without GPS increases, but we note that this decrease is tolerable for our target applications. The data loss stayed relatively stable at 0.21%, even when the global clock source is absent for as long as 5 months. We note that in a densely connected network, the number of paths between any two segments is combinatorial, and hence, the probability of finding a usable path is very high[3]. The variance of the error increased with the length of the gateway's absence.

Dependence on Wake-up Interval: Figures 5(b) show the effect of varying wake-up rate on data loss. As expected, data loss increases as the rate of anchor collection decreases. This curve is strongly related to the segment model: if

[3] One can estimate the probability for finding a usable path using Warshall's algorithm [5]. The input to this algorithm would be a connectivity matrix where the entries represent the anchoring probabilities of the neighbor segments.

collections are less frequent than reboots, many segments will fail to collect enough anchors to be reconstructed.

Robustness: We studied the effect of faulty global clock references on time reconstruction. Noise from a normal distribution ($\mu = 60$ min., $\sigma = 10$ min.) was added to the global references for a period of 128 days. Figure 5(c) shows the alpha and χ values for the GPS mote during the entire simulation period. One can also notice the correlation between high χ values and α values that deviate from 1.0 in Figure 5(c). These faults did not change the data loss rate. The faults increased the PPM error from 4.03 to 16.5. Although these faults decreased accuracy, this decrease is extremely small in comparison to the magnitude of the injected errors and within the targeted accuracy requirements. Phoenix extracted paths which were least affected by these faults by using the χ metric.

Effect of eviction and $NUMSEG$: We studied the effect of $NUMSEG$ on space, duty cycle, and data loss. The space overhead increases linearly with $NUMSEG$ (Figure 6(a)). The impact on duty cycle[4] was quite low (Figure 6(b)). A constant duty cycle penalty of 0.075% is incurred due to the beaconing messages sent every 30 s [15]. At low values of $NUMSEG$, motes are able to switch off their radios early (once they have heard announcements from segments they have anchored with), while at higher values, they need to stay on for the entire T_{listen} period. Increasing $NUMSEG$ decreases data loss, because motes have a better chance of collecting good segments to anchor with. We found that the FCFS eviction policy outperforms LLC and RAND. We found no significant differences in the PPM error results as we vary $NUMSEG$, and hence, we do not report those results here.

Neighbor Density: In this experiment, we removed links from the Cub Hill topology until we obtained the desired neighbor density. At every step, we ensured that the network was fully connected. We did not find any significant impact on performance as the average number of neighbors was decreased. In this experiment, the radios were kept on for the entire T_{listen} period, and no eviction policy was employed. This was done to compare the performance at each density level at the same duty cycle. Figure 6(d) presents our findings.

4.4 Deployment

We deployed a network (referred to as the "Olin" network) of 19 motes arranged in a grid topology in an urban forest near the Johns Hopkins University campus in Baltimore, MD. Anchors were collected for the entire period of 21 days using the methodology described in Section 3.1. The basestation collected data from these motes once every four hours and the NTP-corrected clock of the basestation

[4] Note that the duty cycle that we are referring to does not consider the communication costs during data downloads. Reducing the storage requirements would reduce the communication costs when the basestation collects data.

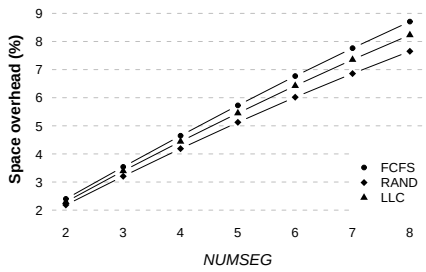

(a) Space overhead in storing anchors as a function of $NUMSEG$.

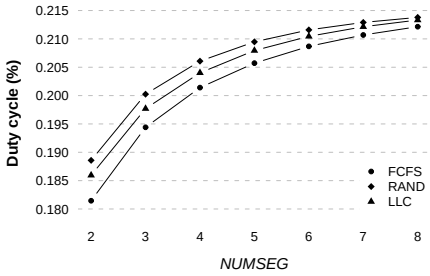

(b) Duty cycle as a function of $NUMSEG$.

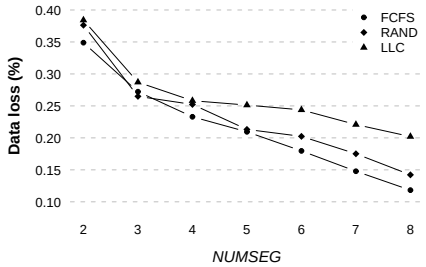

(c) Data loss as a function of $NUMSEG$.

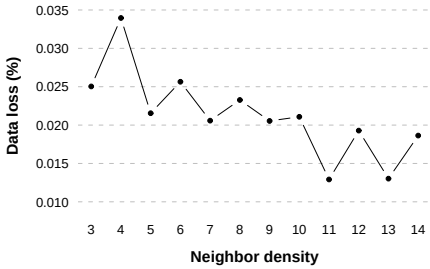

(d) Effect of varying node density on data loss with no eviction policy.

Fig. 6. Effect of $NUMSEG$ on different eviction policies.

was used as a reliable global clock source. The motes rebooted every 5.7 days on average, resulting in a total of 62 segments. The maximum segment length was 19 days and the minimum was two hours.

Perceived Ground Truth: It is very difficult to establish absolute ground truth in field experiments. Instead, we establish a synthetic ground truth by reconstructing timestamps using all the global anchors obtained from the basestation[5]. We record the α and β values for each segment and use these values as ground truth. Because we downloaded data every four hours we obtained enough global anchors from the motes to be confident with the derived ground truth estimates.

Emulating GPS node and Basestation Failure: In order to emulate a GPS mote, we selected a single mote (referred to as G-mote) that was one hop away from the basestation. We used the G-mote's global anchors obtained from the basestation as though they were taken using a GPS device. We ignored all other global anchors obtained from other motes. Furthermore, to emulate the absence of the basestation for N days, we discarded all the anchors taken by the G-mote during that N-day long period. We tested for values of N from one to eighteen.

[5] Note that every time a mote contacts the basestation, we obtain a global anchor for that mote.

Table 1. Phoenix accuracy using the Olin dataset as a function of the number of days that the basestation was unavailable.

Error\Days	2	4	6	8	10	12	14	16	18
α_{med} (ppm)	1.73	1.73	1.85	1.70	1.96	2.20	4.36	5.47	5.93
α_{std} (ppm)	3.41	3.40	3.40	3.39	3.30	3.26	3.17	3.00	3.00
β_{med} (s)	0.88	0.88	0.91	0.94	1.16	1.55	4.52	6.02	6.44
β_{std} (s)	0.58	0.57	0.58	0.57	0.65	0.91	2.43	3.11	3.45

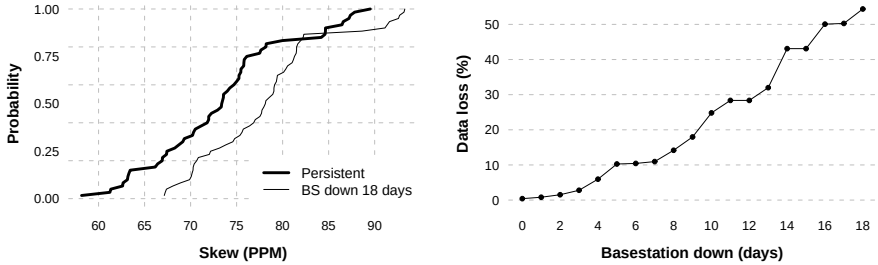

(a) The CDF of α estimates on the Olin deployment

(b) Data loss using RGTR. Data loss from Phoenix was $< 0.06\%$.

Fig. 7. The stability of the α estimates using Phoenix and the data loss using RGTR in comparison to Phoenix.

Phoenix Accuracy: After simulating the basestation failure, we reconstruct the timestamps by applying Phoenix using only the $\langle local, neighbor \rangle$ anchors, and global anchors available from the G-mote. This provides us with another set of α and β estimates for each of the segments. We compare these estimates with the ground truth estimates (pair-wise comparison). In order to provide a deeper insight, we decompose the average PPM error metric into its constituent components - α and β errors. Furthermore, we report the median and standard deviation of these α and β errors. Table 1 reports the results of these experiments. We found that the median α error stayed as low as 5.9 ppm, while the median β error stayed as low as 6.4 s for N =18. In general, α_{med}, β_{med} and β_{std} increased as N increased and α_{std} stayed relatively consistent for different values of N. The stability of the α estimates using Phoenix with $N = 0$ and $N = 18$ is shown in Figure 7(a). The CDF shows that median skew was found to be around 75 ppm and the two curves track each other closely.

Data Loss: The data loss using Phoenix was found to be as low as 0.055% when N was 18 days. In comparison, we found that there was significant data loss when the timestamps were reconstructed using RGTR. Figure 7(b) shows the data losses for different values of N. The figure does not report the Phoenix data loss as we found it to be 0.055% irrespective of N. This demonstrates that Phoenix is able to reconstruct more than 99% of the data even when motes reboot frequently and the basestation is unavailable for days. We note that in

comparison to Phoenix, RGTR does not incur any additional storage and duty cycle overheads as anchors are recorded at the basestation directly as part of the data downloads.

5 Related Work

Assignment of timestamps in sensor networks falls under two broad categories. Strict clock synchronization aims at ensuring that all the mote clocks are synchronized to the same clock source. Flooding Time Synchronization Protocol (FTSP, [13]), Reference Broadcast Synchronization (RBS, [7]), and the Timing-sync Protocol for Sensor Networks [8] are examples of this approach. These systems are typically used in applications such as target tracking and alarm detection which require strong real-time guarantees of reporting events. The second category is known as postmortem time reconstruction and it is mostly used due to its simplicity. While strict synchronization is appropriate for applications where there are specific events of interest that need to be reported, postmortem reconstruction is well-suited for applications where there is a continuous data stream and every measurement requires an accurate timestamp.

Phoenix falls under the second class of methods. The idea of using linear regression to translate local timestamps to global timestamps was first introduced by Werner-Allen et al. in a deployment that was aimed at studying active volcanoes [22]. This work, however, does not consider the impact caused by rebooting motes and basestation failures from a time reconstruction perspective. More recently, researchers have proposed data-driven methods for recovering temporal integrity [9, 10]. Lukac et al. use a model for microseism propagation to time-correct the data collected by their seismic sensors. Although data-driven methods have proved useful for recovering temporal integrity, they are not a solution for accurate timestamping.

Routing integrated time synchronization protocol (RITS, [18]) spans these categories. Each mote along the path (to the basestation) transforms the time of the reported event from the preceding mote's time frame, ending with an accurate global timestamp at the basestation. RITS does not consider the problem of mote reboots, and is designed for target tracking applications. The problem of mote reboots have been reported by a number of research groups. Chang et al. report that nodes rebooted every other day due to an unstable power source [2], whereas Dutta et al. employed the watchdog timer to reboot nodes due to software faults [6]. Allen et al. report an average node uptime of 69% [22]. More recently, Chen et al. advocate *Neutron*, a solution that detects system violations and recovers from them without having to reboot the mote [3]. They advocate the notion of preserving "precious" states such as the time synchronization state. Nevertheless, Neutron cannot prevent all mote reboots and therefore Phoenix is still necessary.

6 Conclusions

In this paper we investigate the challenges facing existing postmortem time reconstruction methodologies due to basestation failures, frequent random mote reboots, and the absence of on-board RTC sources. We present our time reconstruction experiences based on a year-long deployment and motivate the need for robust time reconstruction architectures that minimize data losses due to the challenges we experienced.

Phoenix is an offline time reconstruction algorithm that assigns timestamps to measurements collected using each mote's local clock. One or more motes have references to a global time source. All motes broadcast their time-related state and periodically record the broadcasts of their neighbors. If a few mote segments are able to map their local measurements to the global time frame, this information can then be used to assign global timestamps to the measurements collected by their neighbors and so on. This epidemic-like spread of global information makes Phoenix robust to random mote reboots and basestation failures. We found that in practice there are more than enough possible ways to obtain good fits for the vast majority of data segments.

Results obtained from simulated datasets showed that Phoenix is able to timestamp more than 99% of measurements with an accuracy up to 6 ppm in the presence of frequent random mote reboots. It is able to maintain this performance even when there is no global clock information available for months. The duty-cycle and space overheads were found to be as low as 0.2% and 4% respectively. We validated these results using a 21 day-long real deployment and were able to reconstruct timestamps in the order of seconds.

In the future, we will investigate using other metrics for determining edge weights and their impact on the quality of the time reconstruction. Moreover, we will explore adaptive techniques for determining the anchor collection frequency. Finally, we will derive theoretical guarantees on the accuracy of Phoenix, which can be used to allow for fine-grained tradeoffs between reconstruction quality and overhead.

Acknowledgments

We thank Prabal Dutta, Jay Taneja and the anonymous reviewers for their comments that helped us to improve the paper's presentation. This research was supported in part by NSF grants DBI-0754782 and CNS-0720730. Any opinions, finding, conclusions or recommendations expressed in this publication are those of the authors and do not represent the policy or position of the NSF.

References

1. N. Burri, P. von Rickenbach, and R. Wattenhofer. Dozer: ultra-low power data gathering in sensor networks. In *IPSN*, 2007.

2. M. Chang, C. Cornou, K. Madsen, and P. Bonnet. Lessons from the Hogthrob Deployments. In *WiDeploy*, June 2008.
3. Y. Chen, O. Gnawali, M. Kazandjieva, P. Levis, and J. Regehr. Surviving sensor network software faults. In *SIGOPS*, October 2009.
4. Commonwealth Scientific and Industrial Research Organisation (CSIRO). 2-year progress report: July 2004 to June 2006, 2004.
5. T. H. Cormen, C. E. Leiserson, R. L. Rivest, and C. Stein. *Introduction to Algorithms, Second Edition*. McGraw-Hill Science/Engineering/Math, July 2001.
6. P. Dutta, J. Hui, J. Jeong, S. Kim, C. Sharp, J. Taneja, G. Tolle, K. Whitehouse, and D. Culler. Trio: Enabling sustainable and scalable outdoor wireless sensor network deployments. In *IEEE SPOTS*, pages 407–415, 2006.
7. J. E. Elson, L. Girod, and D. Estrin. Fine-grained network time synchronization using reference broadcasts. In *OSDI*, pages 147–163, Dec. 2002.
8. S. Ganeriwal, R. Kumar, and M. B. Srivastava. Timing-sync protocol for sensor networks. In *Proceedings of SensSys*, pages 138–149, Nov. 2003.
9. J. Gupchup, R. Musaloiu-Elefteri, A. S. Szalay, and A. Terzis. Sundial: Using sunlight to reconstruct global timestamps. In *EWSN*, pages 183–198, 2009.
10. M. Lukac, P. Davis, R. Clayton, and D. Estrin. Recovering temporal integrity with data driven time synchronization. In *IPSN*, pages 61–72, April 2009.
11. L. Luo, C. Huang, T. Abdelzaher, and J. Stankovic. EnviroStore: A cooperative storage system for disconnected operation in sensor networks. In *INFOCOM*, 2007.
12. A. Mainwaring, D. Culler, J. Polastre, R. Szewczyk, and J. Anderson. Wireless sensor networks for habitat monitoring. In *WSNA*, pages 88–97. ACM, 2002.
13. M. Maróti, B. Kusy, G. Simon, and A. Lédeczi. The flooding time synchronization protocol. In *SenSys*, pages 39–49, Nov. 2004.
14. W. A. Marrison. The evolution of the quartz crystal clock. *The Bell System Technical Journal*, 27, 1948.
15. R. Musaloiu-E., C.-J. M. Liang, and A. Terzis. Koala: Ultra-low power data retrieval in wireless sensor networks. In *IPSN*, pages 421–432, 2008.
16. D. Newell and R. Bangert. Temperature compensation of quartz crystal oscillators. In *17th Annual Symposium on Frequency Control. 1963*, pages 491–507, 1963.
17. T. S. Rappaport. *Wireless Communications: Principles and Practice (2nd Edition)*. Prentice Hall PTR, 2 edition, January 2002.
18. J. Sallai, B. Kusy, Á. Lédeczi, and P. Dutta. On the scalability of routing integrated time synchronization. In *EWSN*, volume 3868, pages 115–131. Springer, 2006.
19. J. Taneja, J. Jeong, and D. Culler. Design, modeling, and capacity planning for micro-solar power sensor networks. In *IPSN '08*, pages 407–418, 2008.
20. Texas Instruments Incorporated. MSP430 Datasheet.
21. G. Tolle, J. Polastre, R. Szewczyk, N. Turner, K. Tu, P. Buonadonna, S. Burgess, D. Gay, W. Hong, T. Dawson, and D. Culler. A Macroscope in the Redwoods. In *SenSys*, Nov. 2005.
22. G. Werner-Allen, K. Lorincz, J. Johnson, J. Lees, and M. Welsh. Fidelity and Yield in a Volcano Monitoring Sensor Network. In *OSDI*, Nov. 2006.
23. Y. Yang, L. Wang, D. K. Noh, H. K. Le, and T. F. Abdelzaher. Solarstore: enhancing data reliability in solar-powered storage-centric sensor networks. In *Mobisys*, pages 333–346, New York, NY, USA, 2009. ACM.
24. M. Z. Zamalloa and B. Krishnamachari. An analysis of unreliability and asymmetry in low-power wireless links. *ACM Trans. Sen. Netw.*, 3(2):7, 2007.